analytical chemistry

Article

pubs.acs.org/ac

Highly-Sensitive Amplification-Free Analysis of Multiple miRNAs by Capillary Electrophoresis

David W. Wegman,[†] Farhad Ghasemi,[†] Anna Khorshidi,[‡] Burton B. Yang,[‡] Stanley K. Liu,[§] George M. Yousef,[#] and Sergey N. Krylov*[,†]

[†]Department of Chemistry and Centre for Research on Biomolecular Interactions, York University, 4700 Keele Street, Toronto, Ontario M3J 1P3, Canada

[‡]Department of Laboratory Medicine and Pathobiology, Faculty of Medicine, University of Toronto, 1 King's College Circle, Toronto, Ontario M5S 1A8, Canada

[§]Sunnybrook-Odette Cancer Centre, 2075 Bayview Avenue, Toronto, Ontario M4N 3M5, Canada

[#]Keenan Research Centre, St. Michael's Hospital, 30 Bond Street, Toronto, Ontario M5B 1W8, Canada

Supporting Information

ABSTRACT: Sets of deregulated microRNAs (miRNAs), termed miRNA signatures, are promising biomarkers for cancer. Validation of miRNA signatures requires a technique that is accurate, sensitive, capable of detecting multiple miRNAs, fast, robust, and not cost-prohibitive. Direct quantitative analysis of multiple miRNAs (DQAMmiR) is a capillary electrophoresis (CE)-based hybridization assay that was suggested as a methodological platform for validation and clinical use of miRNA signatures. While satisfying the other requirements, DQAMmiR is not sufficiently sensitive to detect low-abundance miRNAs. Here, we solve this problem by combining DQAMmiR with the preconcentration technique, isotachophoresis (ITP). The sensitivity improved 100 times (to 1 pM) allowing us to detect low-abundance miRNAs in an RNA extract. Importantly, ITP-DQAMmiR can be performed in a fully automated mode using a commercial CE instrument making it suitable for practical applications.

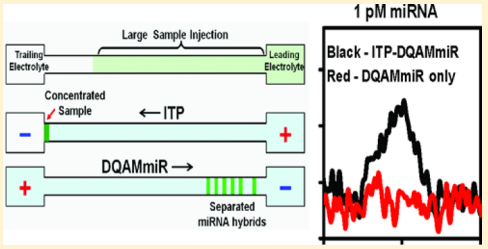

miRNAs are short RNA sequences (18−25 nucleotides long) that regulate gene expression. Abnormal levels of miRNAs in pathological tissues, such as tumors, make them a promising class of biomarkers for diagnostic and prognostic purposes.[1,2] The identification of potential miRNA signatures can be performed on a relatively small number of samples by using microarrays, a semiquantitative approach capable of analyzing thousands of miRNAs simultaneously.[3] The validation of miRNA signatures, however, requires very accurate quantitative analysis of relatively few miRNAs in thousands of samples. Quantitative analysis of miRNAs is also essential for stoichiometric comparisons of miRNA versus exosomes[4] or when working with very small quantities of miRNAs such as blood plasma[5] or fine-needle biopsies.[6] The analysis of thousands of samples can often only be done by cooperation of many laboratories and requires an analytical technology that is not only accurate, sensitive, and capable of detecting multiple miRNAs but is also fast, robust, and not cost-prohibitive. None of the currently used miRNA detection techniques satisfy all these conditions. Of the most commonly used techniques, both quantitative reverse transcriptase polymerase chain reaction (qRT-PCR) and next-generation sequencing are prone to amplification-related errors and the latter is also time-consuming and prohibitively expensive in materials.[7−11] NanoString technology may not be sensitive enough for detection of down-regulated miRNAs, is time-consuming (2 days), and requires very costly consumables.[12−14] Thus, there has been a continuing effort to create new methodological platforms that could satisfy the stringent requirements of miRNA signature validation.[15−27]

Among the new platforms is Direct Quantitative Analysis of Multiple miRNAs (DQAMmiR), a capillary electrophoresis (CE)-based hybridization assay.[27] In any electrophoresis-based assay of multiple miRNAs, excess of DNA hybridization probes, labeled for detection, is reacted with the sample to ensure that all miRNA targets are hybridized. A fundamental problem in such an approach is the need to separate unreacted probes from hybrids and hybrids of different miRNAs from each other. In DQAMmiR, these problems are solved by using two types of mobility shifters: (1) single-strand DNA binding protein (SSB) is added to the run buffer to separate the unreacted probes, and (2) drag tags of varying size are covalently attached to the DNA hybridization probes to separate different hybrids. The concept of DQAMmiR is depicted in Figure 1A with details described in the figure legend for convenience. DQAMmiR is a calibration-free technique that measures absolute amounts of multiple miRNAs in a straightforward way, allowing it to be robust toward differences in instrumentation used. The DQAMmiR

Received: November 25, 2014
Accepted: December 13, 2014
Published: December 13, 2014

DOI: 10.1021/ac504406s
Anal. Chem. 2015, 87, 1404−1410

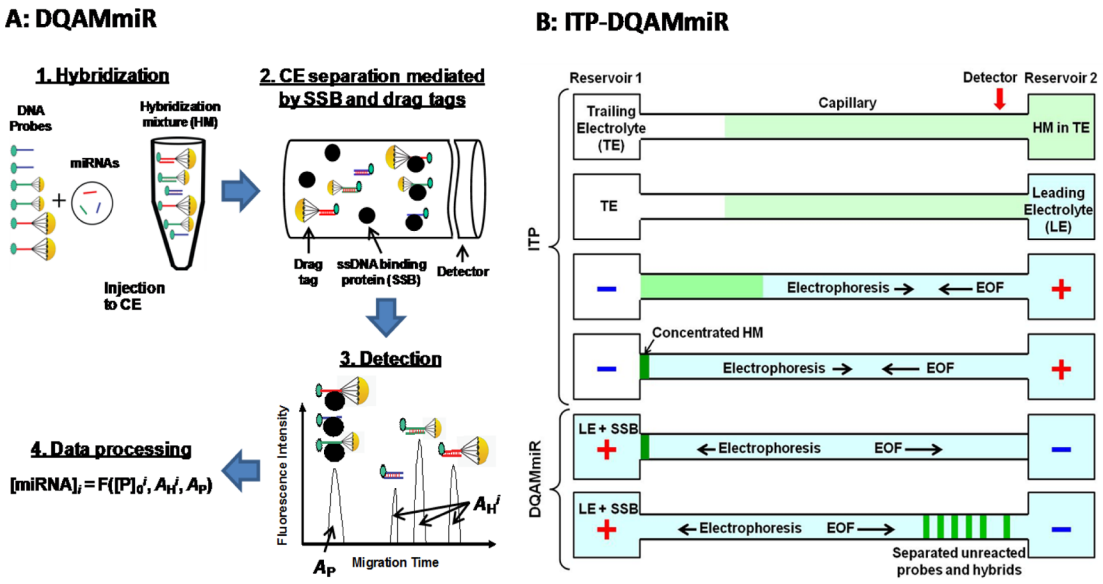

Figure 1. Conceptual depiction of (A) direct quantitative analysis of multiple miRNAs (DQAMmiR) and (B) streamlined combination of isotachophoresis (ITP) and DQAMmiR. In panel A, the miRNAs and complementary ssDNA in hybridization probes are shown as short lines of the same color, drag tags are shown as parachutes, fluorescent labels are shown as small green circles, and SSB is shown as a large black circle. In step 1, an excess of the probes is mixed with the miRNAs and incubated to prepare a hybridization mixture (HM) in which all miRNAs are hybridized but some probes are left unreacted. In step 2, a short plug of HM is introduced into a capillary with an SSB-containing run buffer. SSB binds all ssDNA probes but does not bind the double-stranded miRNA−DNA hybrid. When an electric field is applied, all SSB-bound probes move faster than all the hybrids (SSB works as a propellant). On the other hand, different drag tags make different hybrids move with different velocities. In step 3, a fluorescent detector at the end of the capillary generates separate signals for the hybrids and unreacted probes. In step 4, the concentrations of the different miRNAs are determined from integrated signals (peak areas in the graph) by a simple mathematical approach that requires the knowledge of total concentration of all the probes, $[P]_0^i$ and peak areas corresponding to all probes, A_P, and individual hybrids, A_H^i. In panel B, the major stages of the ITP-DQAMmiR tandem analysis are shown. In the ITP stage, the capillary is prefilled with a trailing electrolyte (TE) of low conductivity by a pressure-driven flow from Reservoir 1. HM is prepared in TE and a large predetermined part of the capillary is filled with HM by a pressure-driven flow from Reservoir 2 (detection end of the capillary). HM in Reservoir 2 is replaced with a leading electrolyte (LE) with high conductivity and a voltage is applied with the positive electrode being in Reservoir 2. The electroosmotic flow (EOF) from the positive to the negative electrode is faster than the electrophoretic migration of the hybrids and probes in the opposite direction. This leads to the concentration of probes and hybrids inside the capillary near Reservoir 1. In the DQAMmiR stage, TE in Reservoir 1 is replaced with SSB-containing LE. The voltage is now applied with the positive electrode being in Reservoir 1. Continuously supplied SSB migrates faster than the probes and hybrids and overruns them. The latter facilitates SSB-driven separation of the unreacted probes from the hybrids.

analysis can be optimized to take only 20 min which is much faster than any other available method.[28] The assay is not affected by the presence of a crude cell lysate and is thus robust toward variations in sample preparation quality.[27] DQAMmiR is capable of simultaneous analysis of 5 miRNAs, and this number can be extended to 20−30 by using peptides of varying lengths as drag tags.[29] The per-assay cost of consumables in DQAMmiR is under $5 even for their current small-scale production. This is 10−100 times less than the per-assay costs of consumables used in analyses of miRNA by qRT-PCR, NanoString, microarrays, and next-generation sequencing. The only requirement that DQAMmiR does not meet is high sensitivity or, more specifically, low concentration limit of detection (LOD). The concentration LOD of DQAMmiR using the most sensitive commercial CE instrument available is 100 pM of miRNA, which is insufficient to detect low-abundance miRNAs.[27] Further efforts showed that decreasing concentration LOD through improving a fluorescence detector requires considerable development.[30] Therefore, to bring DQAMmiR closer to a practical approach for validation of miRNA signatures, we explored sample preconcentration as a potential solution.

The requirement of keeping DQAMmiR's suitability for automation limits us to preconcentration inside the capillary. Isotachophoresis (ITP) is an electrophoretic separation technique which can be used for analyte concentration.[23,24,31−33] It utilizes the fact that ions move with different velocities in buffers with different conductivities. In preconcentration by ITP, a large fraction of the capillary is filled with the sample sandwiched between the high-conductivity leading electrolyte (LE) and the low-conductivity trailing electrolyte (TE). When an electric field is applied, the analytes focus on the interface between LE and TE. Santiago's group suggested the use of ITP for miRNA analysis in a chip format with an impressive concentration LOD of 5 pM.[23] Even though their approach was only applicable to the analysis of a single miRNA,[23−25] it motivated our attempt to combine ITP preconcentration with DQAMmiR. Our goal was to develop streamlined ITP-DQAMmiR which first preconcentrates multiple hybrids and unreacted probes by ITP and then separates the probes from the hybrids and hybrids from each other using DQAMmiR. Figure 1B depicts all essential steps of ITP-DQAMmiR with details described in the figure legend for convenience. We were able to successfully preconcentrate, separate, and detect multiple miRNA in a single capillary, using a commercial instrument with no manual steps required.

EXPERIMENTAL SECTION

Hybridization Probes. All miRNA and hybridization probes were custom-synthesized by IDT (Coralville, IA). To

DOI: 10.1021/ac504406s
Anal. Chem. 2015, 87, 1404−1410

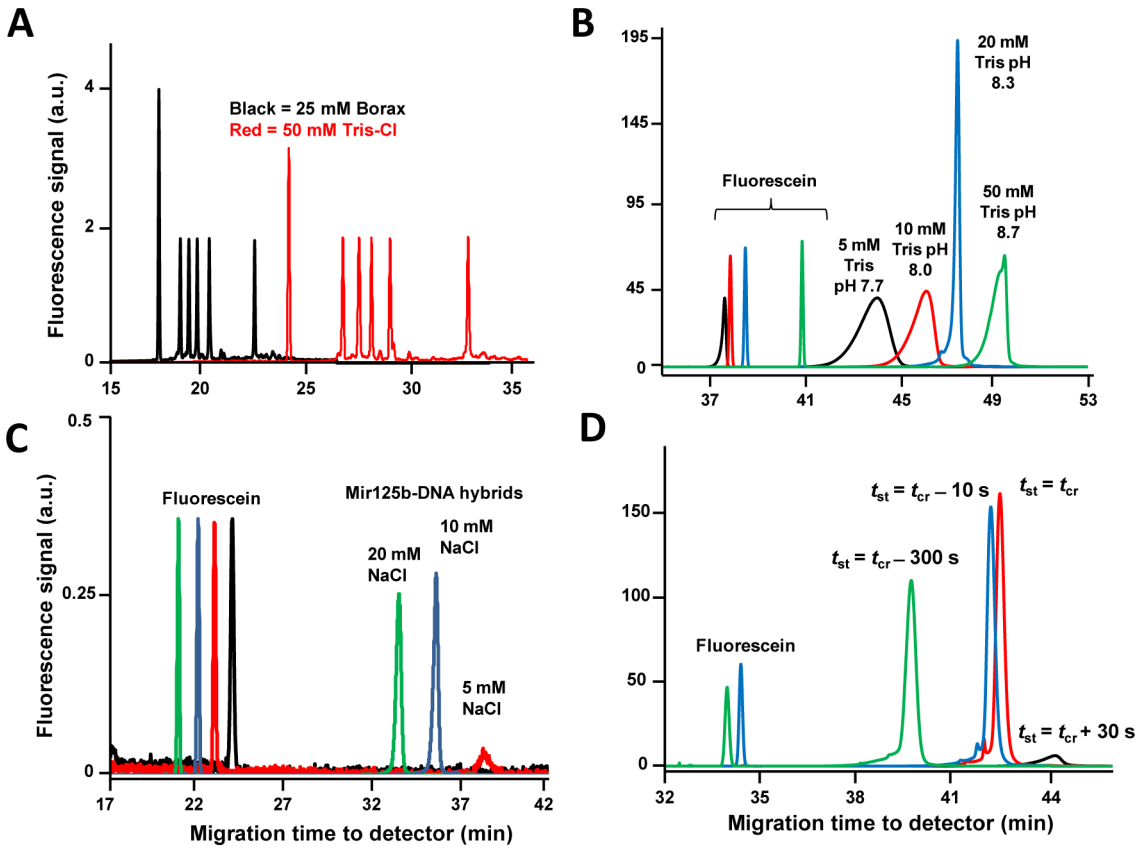

Figure 2. Optimization of: composition, concentration, and pH of LE and TE (A–C) and ITP stop time (D). Panel A compares the resolution of multiple peaks in DQAMmiR runs (without ITP) with either original DQAMmiR electrolyte (25 mM Borax) or LE (50 mM Tris-Cl). The sample for each run contained 10 nM fluorescein (left peak) and 5 nM of five DNA probes with peptide drag tags of 20, 15, 10, 5, and 0 amino acids in length, respectively, from left to right. The resolution of peaks was similar to both buffers. Panel B illustrates the effect of the concentration and pH of TE (Tris-HEPES) on the EOF-mediated analyte dispersion manifested by peak broadening. After injecting a sample containing 1 nM fluorescein and 10 nM miR125b DNA probe into the capillary, ITP-DQAMmiR was performed. The greatest resolution and narrowest peaks were observed with Tris-HEPES (20 mM Tris and 10 mM HEPES), pH 8.3. Panel C illustrates the determination of the minimum NaCl concentration required in incubation buffer to prevent SSB-mediated hybrid dissociation. A range of NaCl concentrations (0–100 nM) were added to TE and used as the incubation buffer for the hybridization mixture. SSB-mediated DQAMmiR was performed with a sample containing 10 nM miR125b DNA probe, 1 nM miR125b, and 1 nM fluorescein, and hybrid peak areas were assessed. The minimum NaCl concentration that prevented hybrid dissociation (manifested by decreasing hybrid peak area) was 10 mM. To note, the black trace contains 0 mM NaCl and did not produce a hybrid peak. Hybrid peaks for NaCl concentrations higher than 20 mM were not observed due to the disruption of the ITP process (the hybrid could not reach the detection end of the capillary). Panel D illustrates the determination of optimum ITP stop time (t_{st}), the time point at which the concentrated sample nears the end of the capillary and maximum resolution is achieved without any loss of sample. We varied t_{st} with respect to the "critical" point (t_{cr}), the time-point at which the current versus time slope abruptly changes to zero. Using a sample containing 1 nM fluorescein and 10 nM miR125b DNA probe we found that $t_{st} = t_{cr} - 10$ s had the greatest resolution without the loss of DNA or fluorescein (as observed in the $t_{st} = t_{cr}$ run).

allow separation of the five hybrid peaks, peptide drag tags of varying size were conjugated to the DNA probes via a thioether bond. The conjugation reaction, which is described in our previous work,[29] occurs between a thiol group on the 5′ end of the DNA probes and a maleimide group on the N terminus of each peptide. All maleimide modified peptides were synthesized by Canpeptide (Pointe-Clare, QUE, Canada). All miRNA, DNA probe and peptide sequences can be found in Table S1 in the Supporting Information.

Hybridization Conditions. Hybridization was carried out in a Mastercycler 5332 thermocycler (Eppendorf, Hamburg, Germany). Various concentrations of the five miRNA species (miR10b, miR21 miR125b, miR145, miR155) were incubated with 5 nM of their respective DNA probes along with 1 nM fluorescein (internal standard) and 10 nM Masking RNA in TE-hybridization buffer (20 mM Tris, 10 mM HEPES, 10 mM NaCl, pH 8.3). The masking RNA was a tRNA library from baker's yeast from Sigma-Aldrich (Oakville, ON, Canada). Temperature was increased to a denaturing 80 °C and then lowered to 37 °C at a rate of 20 °C/min and was held at 37 °C for 1 h to allow annealing. To minimize miRNA degradation, a nuclease-free environment was used while handling miRNA samples.

ITP-DQAMmiR. We used a P/ACE MDQ capillary electrophoresis system (Beckman-Coulter, Fullerton, CA) with laser-induced fluorescence detection. We used bare fused-silica capillaries with an outer diameter of 365 μm, an inner diameter of 75 μm, and a total length of 79.4 cm. The distance from the end of the capillary in Reservoir 1 (Figure 1B) to the detector was 69 cm. The capillary was flushed prior to every CE run with 0.1 M HCl, 0.1 M NaOH, deionized H_2O, and TE buffer (20 mM Tris, 10 mM HEPES, pH 8.3) for 1 min each. Samples were injected from Reservoir 2 by a pressure pulse of 3.0 psi for 99 s. The volume of the injected sample was

DOI: 10.1021/ac504406s
Anal. Chem. 2015, 87, 1404–1410

1.9 μL. The buffer in Reservoir 2 was switched to LE buffer (50 mM Tris-Cl, 10 mM NaCl, pH 8.0) and electric field was applied in the reverse direction. Electrophoresis was driven by an electric field of 312.5 V/cm. The voltage was turned off at t_{cr} − 10 s, where t_{cr} is the predetermined "critical time-point" explained in the Results and Discussion. The buffer in Reservoir 1 was switched to LE + 50 nM SSB and an electric field of 312.5 V/cm was applied in the forward direction. When the samples passed the detector, the fluorescence was excited with a 488 nm continuous wave solid-state laser (JDSU, Santa Rosa, CA). Electropherograms were analyzed using 32 Karat Software. Peak areas were divided by the corresponding migration times to compensate for the dependence of the residence time in the detector on the electrophoretic velocity of species. Concentrations of miRNA were determined using the following equation.

$$[\text{miRNA}]_i = \frac{A_{H,i}}{A_P + \sum_{j=1}^{N}(q_{P,j}/q_{H,j})A_{H,j}} \left(\sum_{j=1}^{N}(q_{P,j}/q_{H,i})[P]_{0,j}\right)$$

where $[P]_{0,j}$ is the total concentration of the j-th probe (composed of the hybrid and the miRNA-unbound probe), A_H is the area corresponding to the i-th or j-th hybrid, A_P is the cumulative area of the excess probe, q_H is the relative quantum yield of the i-th or j-th hybrid with respect to that of the free probe, $q_{P,j}$ is the relative quantum yield of the j-th probe in the presence of SSB with respect to that of the free probe, and N is the total number of DNA probes. In this equation we assume that all target miRNA are hybridized. Derivation of the equation can be found in the Supporting Information. Quantum yields can be found in Tables S2−S4 in the Supporting Information.

MCF-7 RNA Extraction. MCF-7 cells were purchased from ATCC and grown in an incubator at 37 °C in the atmosphere of 5% CO_2. Cells were grown in RPMI 1640 media (Wisent Inc., Saint-Jean-Baptiste, QUE, Canada) plus 10% FBS and 1% penicillin, streptomycin in a 100 mm Petri dish. When cells covered roughly 90% of the plate they were washed with PBS, trypsinized to detach them from the bottom of the dish and centrifuged at 150*g* for 5 min. The pellet was washed twice with PBS. The cells were counted using a hemocytometer, and the mirVANA miRNA isolation kit (Ambion, Austin, TX) was used to extract the RNA according to the manufacturer's instructions. Extracted RNA was aliquoted and stored at −80 °C. Hybridization, injection, and ITP-DQAMmiR were performed as previously explained.

Determination of miRNA Concentration Using UV Absorbance. For Figure 4, the "Actual concentration" of the target miRNA was determined using UV absorbance. The light absorbance for each miRNA stock solution was measured at 260 nm using the Nano-Drop ND-1000 spectrophotometer (Thermo-Fisher Scientific, Waltham, MA). The concentration was calculated using Beer's Law, and the the miRNA's molar extinction coefficient was provided by IDT.

RESULTS AND DISCUSSION

For ITP-DQAMmiR to work, its multiple steps shown in Figure 1B must be smoothly interfaced by choosing proper compositions, concentrations, and pH of LE and TE. Five requirements should be satisfied: (i) there should be no buffer mismatch between the final step in ITP and initial step in DQAMmiR, (ii) ITP should preconcentrate all components of HM into a single narrow zone, (iii) electro-osmotic flow (EOF)-mediated analyte dispersion must be limited, (iv) SSB-mediated hybrid dissociation must be limited, and (v) the ITP step must be stopped when the concentrated HM reaches the end of the capillary.

First, to avoid buffer mismatch, we required a LE for ITP that could also be used as the electrolyte in DQAMmiR. Matching the LE with the DQAMmiR run buffer turned out to be an easy task. Tris-Cl, which is a very common LE in ITP, is also often used for CE separation. Our attempt to use Tris-Cl as the run buffer in DQAMmiR was successful, as shown by the separation of 5 DNA probes with a resolution comparable to our previous work (Figure 2A).

Second, preconcentration of multiple analytes into a single narrow band requires that (i) the concentration of LE (and TE) be much greater than the cumulative concentration of all the analytes and (ii) the mobility difference between LE and TE is maximized.[34] Considering that the DNA probe and miRNA concentrations are in the pM to nM range, the first requirement can be easily satisfied by using LE and TE concentrations in the mM range. Since we have already chosen Tris-Cl as an LE, satisfying the second requirement depended solely on the choice of TE, the mobility of TE should be as low as possible. Tris-HEPES is known to have a lower mobility than most other TE buffers used with ITP of nucleic acids.[35] With the use of mM amounts of Tris-Cl and Tris-HEPES as LE and TE, respectively, we successfully preconcentrated all target analytes, observed by the single, narrow peak in an ITP-only run (Figure S1 in the Supporting Information).

Third, with our chosen buffers we required optimum pH and ionic strengths that would limit any ITP disruption and dispersion by EOF. Slight changes in pH and ionic strength of the buffers not only affect ITP focusing but can also affect the EOF velocity, changing the effective length of ITP separation and potentially causing analyte dispersion.[34] Thus, by varying concentration within the predetermined mM range and pH within the Tris buffering range (pK_a = 8.2) we were able to find the optimum conditions for preconcentration of multiple analytes by ITP (Figure 2B and Figure S2 in the Supporting Information).

Fourth, SSB has the ability to dissociate weakly bound hybrids especially in low-ionic-strength buffers.[36] Thus, in DQAMmiR, the incubation buffer (20 mM Tris, 10 mM HEPES, pH 8.3) must include a sufficient concentration of salt to stabilize the hybrid. The inclusion of extra salt (NaCl in our case), on the other hand, alters the conductivity of the buffers and our challenge was to introduce NaCl without affecting ITP preconcentration. To maintain optimum preconcentration by ITP, we needed to find the minimum required concentration of NaCl that would prevent SSB-mediated hybrid dissociation. We included a range of NaCl concentrations (0−100 mM) to the incubation buffer (IB) and ran SSB-mediated CE to test if the hybrid peak was present (Figure 2C). The minimum concentration of NaCl in IB that maintained hybrid integrity was 10 mM. NaCl was only added to IB and LE as adding chloride ion (leading electrolyte) in TE buffer disrupts the ITP process and results in peak broadening (Figure S3 in the Supporting Information).

Fifth and final, in ITP-DQAMmiR, the preconcentrated HM should be stopped before leaving the capillary so that the following separation of its components in the opposite

DOI: 10.1021/ac504406s
Anal. Chem. 2015, 87, 1404−1410

direction could be accomplished (Figure 1B). Our task was to find a way to stop ITP in a robust fashion before the concentrated sample leaves the capillary with as little residual TE remaining as possible as it could deteriorate the quality of CE separation. After exploring a number of options, we focused on the value of electrical current as an indicator of ITP stop time, t_{st} similar to Reinhoud's work in the early 90s.[37] The displacement of TE with LE during ITP is accompanied by gradually increasing the electrical current. There is a "critical" point, t_{cr}, on the current versus time dependence where the slope abruptly changes from finite to zero (Figure S4 in the Supporting Information). This time likely corresponds to the moment of the completion of electrolyte displacement. Importantly, t_{cr} was very stable; its deviation was only 0.4% or 4 s. We thus decided to relate t_{st} to this critical point. We studied how stopping ITP at different times $t_{st} = t_{cr} \pm x$, where x varied between −60 and +60 s with an increment of 5 s, would influence resolution between the fluorescein peak and miR125b DNA probe peak. We wanted to find the optimum ITP time, defined as the time at which maximum peak resolution occurs without the loss of any sample. ITP times considerably (30 s) shorter than t_{cr} led to lowered resolution while longer ITP times led to HM elution from the capillary and loss of target analytes. We found that stopping ITP at $t_{st} = t_{cr} - 10$ s achieved maximum resolution without the loss of any target analytes (Figure 2D). We used $t_{st} = t_{cr} - 10$ s to automatically stop ITP and start CE separation by changing the polarity. The observed consistency of the optimum ITP time using different capillaries (of the same length) on different days (Table S1 in the Supporting Information), allowed for the automation of this process.

After resolving the challenges of combining ITP with DQAMmiR, we could study the performance of ITP-DQAMmiR. The first aspect to assess was the concentration LOD, defined as the miRNA concentration at which the respective hybrid peak signal is at a 3 to 1 ratio to the background noise. We compared peaks of a hybrid for DQAMmiR and ITP-DQAMmiR. The minimum concentration of miRNA that could be detected by DQAMmiR was 100 pM while ITP-DQAMmiR could detect as low as 1 pM miRNA (Figure 3). Slight differences in DNA probe fluorescent intensity prevented all miRNA from achieving 1 pM LOD; however, they all achieved an LOD of 5 pM or lower. Thus, with ITP-DQAMmiR, we were able to improve the LOD 100 times in comparison to the LOD of DQAMmiR alone with only a 35 min increase in overall assay time. The 100 times improvement was consistent with the increase in HM volume injected; in DQAMmiR it was 14 nL while in ITP-DQAMmiR it was 1.9 μL. This suggests that increasing the capillary length can lead to even lower LODs, though this would inherently be linked with an increase in total assay time.

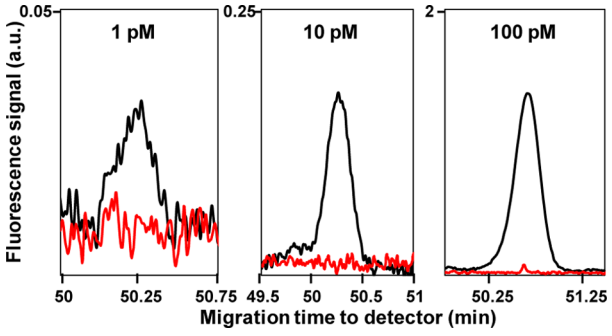

Figure 3. Comparison of limit of detection between DQAMmiR (red trace) and ITP-DQAMmiR (black trace). Each peak represents the hybrid of varying miR125b concentrations (1, 10, and 100 pM) with 5 nM of its respective DNA probe. DQAMmiR could only detect 100 pM miR125b while ITP-DQAMmiR detected 1 pM miR125b, a 100 times improvement.

The second aspect investigated was the accurate quantitation of multiple miRNA in ITP-DQAMmiR. Interestingly, the resolution between hybrid peaks achieved with ITP-DQAMmiR (Figure 4A) was greater than the resolution achieved with

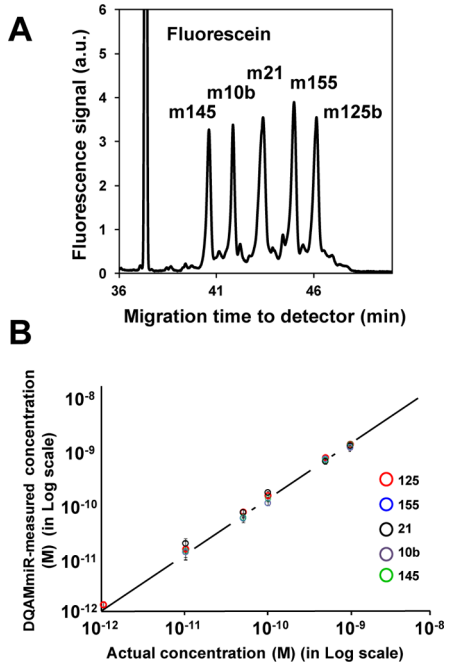

Figure 4. Separation, detection, and quantitation of 5 miRNA species. Panel A shows the detection of 5 DNA−miRNA hybrid peaks, along with the internal standard, fluorescein using ITP-DQAMmiR. All hybrid peak areas were normalized by their respective quantum yields (Tables S3−S5, Supporting Information). Panel B Quantitative analysis of 1 pM to 1 nM of all 5 miRNA (miR-125b, 155, 21, 10b, and 145), with error bars included. Concentrations of miRNA were validated by light absorbance of the miRNA stock solution at 260 nm. Each data point is based on three measurements. Error bars represent a standard deviation.

DQAMmiR (Figure S5 in the Supporting Information). Such excellent resolution potentially allows ITP-DQAMmiR to simultaneously detect up to 21 miRNA. As a proof of principle, the separation of five distinct hybrid peaks allowed us to accurately quantitate 5 miRNA species over a dynamic range of 1 to 1000 pM (Figure 4B). Thus, we were able to accurately quantitate multiple miRNA in the low pM range without affecting dynamic range.

Finally, we applied ITP-DQAMmiR to the analysis of multiple miRNAs from a biological sample. In our previous work,[27] we were only able to detect the highly abundant miR21, whose peak was close to our limit of detection. With ITP-DQAMmiR our goal was to shift the dynamic range to allow the detection of low abundance miRNA while still being able to detect the highly abundant miRNA without oversaturation of our detectors. We achieved this which is demonstrated by simultaneously detecting highly abundant (miR21) and low

DOI: 10.1021/ac504406s
Anal. Chem. 2015, 87, 1404−1410

abundance (miR155 and miR125b) miRNA[1,38,39] from a MCF-7 RNA extract sample (Figure 5). With the low-abundance

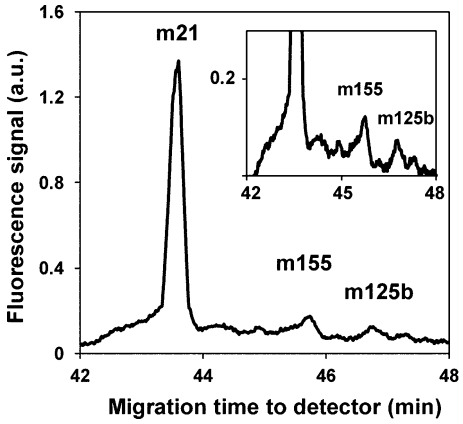

Figure 5. Detection of multiple miRNA from a biological sample using ITP-DQAMmIR. An MCF-7 RNA extract was incubated with 5 nM of the respective probes for miR125b, miR155, and miR21. ITP-DQAMmiR was performed as previously explained. Both the highly abundant miR21 and low abundance miR155 and miR125b were detected in the same run.

miRNA close to our limit of detection and the miR21 peak not oversaturated, it shows that we can now detect low, mid, and high abundance miRNA simultaneously. Known concentrations of the three miRNA were spiked into the RNA extract samples to account for any effects the RNA extract matrix had on quantification, which was found to be negligible (Figure S6 in the Supporting Information). The ability to detect the majority of miRNA species shows that ITP-DQAMmiR is one step closer to its use in the validation of miRNA signatures. Such signatures (tentative) are selected from large sets of miRNAs. Essentially, the choice of miRNA for a tentative signature would depend on whether or not we can reliably detect it. Since we can now detect a large range of biologically relevant concentrations, it makes it much easier to choose the miRNA for the tentative fingerprint.

CONCLUSIONS

To conclude, we have demonstrated the successful combination of ITP and DQAMmiR in a single capillary using a commercial instrument for simultaneous analysis of multiple miRNAs. This allows for the fully automated preconcentration, separation, and quantitation of multiple miRNA in a single experiment. We were able to detect miRNA amounts in the low pM range with an LOD of 1 pM, which is a 100-time improvement over the best previous result with DQAMmiR.[27] We have optimized a compatible set of buffers which allowed for both ITP and DQAMmiR to be performed without hindrance. The ability to preconcentrate and separate multiple miRNAs makes ITP-DQAMmiR a viable method for use in the validation of miRNA signatures.

ASSOCIATED CONTENT

Supporting Information

Supporting materials and methods, supporting results, and supporting mathematics. This material is available free of charge via the Internet at http://pubs.acs.org.

AUTHOR INFORMATION

Corresponding Author

*E-mail: skrylov@yorku.ca.

Author Contributions

The manuscript was written through contributions of all authors. All authors have given approval to the final version of the manuscript.

Notes

The authors declare no competing financial interest.

ACKNOWLEDGMENTS

We thank Canadian Institutes of Health Research and Natural Sciences and Engineering Research Council of Canada.

REFERENCES

(1) Iorio, M. V.; Ferracin, M.; Liu, C.-G.; Veronese, A.; Spizzo, R.; Sabbioni, S.; Magri, E.; Pedriali, M.; Fabbri, M.; Campiglio, M.; Menard, S.; Palazzo, J. P.; Rosenberg, A.; Musiani, P.; Volinia, S.; Nenci, I.; Calin, G. A.; Querzoli, P.; Negrini, M.; Croce, C. M. *Cancer Res.* **2005**, *65*, 7065−7070.

(2) Youssef, Y. M.; White, N. M.; Grigull, J.; Krizova, A.; Samy, C.; Mejia-Guerrero, S.; Evans, A.; Yousef, G. M. *Eur. Urol.* **2001**, *9*, 721−730.

(3) Liu, C.-G.; Calin, G. A.; Meloon, B.; Gamliel, N.; Sevignani, C.; Ferracin, M.; Dumitru, C. D.; Shimizu, M.; Zupo, S.; Dono, M.; Alder, H.; Bullrich, F.; Negrini, M.; Croce, C. M. *Proc. Natl. Acad. Sci. U.S.A.* **2004**, *101*, 9740−9744.

(4) Chevillet, J. R.; Kang, Q.; Ruf, I. K.; Briggs, H. A.; Vojtech, L. N.; Hughes, S. M.; Cheng, H. H.; Arroyo, J. D.; Meredith, E. K.; Gallichotte, E. N.; Pogosova-Agadjanyan, E. L.; Morrissey, C.; Stirewalt, D. L.; Hladik, F.; Yu, E. Y.; Higano, C. S.; Tewari, M. *Proc. Natl. Acad. Sci. U.S.A.* **2014**, *111*, 14888−14893.

(5) Ma, J.; Li, N.; Guarnera, M.; Jiang, F. *Biomarker Insights* **2013**, *8*, 127−136.

(6) Roskell, D. E.; Buley, I. D. *BMJ* **2004**, *329*, 244−245.

(7) Lao, K.; Xu, N. L.; Yeung, V.; Chen, C.; Livak, K. J.; Straus, N. A. *Biochem. Biophys. Res. Commun.* **2006**, *343*, 85−89.

(8) Morin, R. D.; O'Connor, M. D.; Griffith, M.; Kuchenbauer, F.; Delaney, A.; Prabhu, A.-L.; Zhao, Y.; McDonald, H.; Zeng, T.; Hirst, M.; Eaves, C. J.; Marra, M. A. *Genome Res.* **2008**, *18*, 610−621.

(9) Ohtsuka, E.; Nishikawa, S.; Fukumoto, R.; Tanaka, S.; Markham, A. F.; Ikehara, M.; Sugiura, M. *Eur. J. Biochem.* **1977**, *81*, 285−291.

(10) McLaughlin, L. W.; Romaniuk, E.; Romaniuk, P. J.; Neilson, T. *Eur. J. Biochem.* **1982**, *125*, 639−643.

(11) Weiss, E. A.; Gilmartin, G. M.; Nevins, J. R. *EMBO J.* **1991**, *10*, 215−219.

(12) Knutsen, E.; Fiskaa, T.; Ursvik, A.; Jørgensen, T. E.; Perander, M.; Lund, E.; Seternes, O. M.; Johansen, S. D.; Andreassen, M. *PLoS One* **2013**, *8*, e75813.

(13) Kolbert, C. P.; Feddersen, R. M.; Rakhshan, F.; Grill, D. E.; Simon, G.; Middha, S.; Jang, J. S.; Simon, V.; Schultz, D. A.; Zschunke, M.; Lingle, W.; Carr, J. M.; Thompson, E. A.; Oberg, A. L.; Eckloff, B. W.; Wieben, E. D.; Li, P.; Yang, P.; Jen, J. *PLoS One* **2013**, *8*, e52517.

(14) Geiss, G. K.; Bumgarner, R. E.; Birditt, B.; Dahl, T.; Dowidar, N.; Dunaway, D. L.; Fell, H. P.; Ferree, S.; George, R. D.; Grogan, T.; James, J. J.; Maysuria, M.; Mitton, J. D.; Oliveri, P.; Osborn, J. L.; Peng, T.; Ratcliffe, A. L.; Webster, P. J.; Davidson, E. H.; Hood, L. *Nat. Biotechnol.* **2008**, *26*, 317−325.

(15) Zheng, W.; Chase, T. E.; He, L. *Anal. Methods* **2014**, *6*, 2399−2405.

(16) Zhang, P.; Zhang, J.; Wang, C.; Liu, C.; Wang, H.; Li, Z. *Anal. Chem.* **2013**, *86*, 1076−1082.

(17) Zhang, P.; Liu, Y.; Zhang, Y.; Liu, C.; Wang, Z.; Li, Z. *Chem. Commun.* **2013**, *49*, 10013−10015.

(18) Ho, S.-L.; Chan, H.-M.; Wong, R. N.-S.; Li, H.-W. *Anal. Chim. Acta* **2014**, *823*, 61−68.

DOI: 10.1021/ac504406s
Anal. Chem. 2015, 87, 1404−1410

(19) Ban, E.; Chae, D.-K.; Song, E. J. *J. Chromatogr., A* **2013**, *1315*, 195−199.
(20) Zhang, G.-J.; Chua, J. H.; Chee, R.-E.; Agarwal, A.; Wong, S. M. *Biosens. Bioelectron.* **2009**, *24*, 2504−2508.
(21) Cissell, K. A.; Rahimi, Y.; Shrestha, S.; Hunt, E. A.; Deo, S. K. *Anal. Chem.* **2008**, *80*, 2319−2325.
(22) Neely, L. A.; Patel, S.; Garver, J.; Gallo, M.; Hackett, M.; McLaughlin, S.; Nadel, M.; Harris, J.; Gullans, S.; Rooke, J. *Nat. Methods* **2006**, *3*, 41−46.
(23) Bahga, S. S.; Santiago, J. G. *Analyst* **2013**, *138*, 735−754.
(24) Garcia-Schwarz, G.; Santiago, J. G. *Anal. Chem.* **2012**, *84*, 6366−6369.
(25) Garcia-Schwarz, G.; Santiago, J. G. *Angew. Chem., Int. Ed.* **2013**, *52*, 11534−11537.
(26) Khan, N.; Cheng, J.; Pezacki, J. P.; Berezovski, M. V. *Anal. Chem.* **2011**, *83*, 6196−6201.
(27) Wegman, D. W.; Krylov, S. N. *Angew. Chem., Int. Ed.* **2011**, *50*, 10335−10339.
(28) Ghasemi, F.; Wegman, D. W.; Kanoatov, M.; Yang, B. B.; Liu, S. K.; Yousef, G. M.; Krylov, S. N. *Anal. Chem.* **2013**, *85*, 10062−10066.
(29) Wegman, D. W.; Cherney, L. T.; Yousef, G. M.; Krylov, S. N. *Anal. Chem.* **2013**, *85*, 6518−6523.
(30) Dodgson, B. J.; Mazouchi, A.; Wegman, D. W.; Gradinaru, C. C.; Krylov, S. N. *Anal. Chem.* **2012**, *84*, 5470−5474.
(31) Bočker, P.; Gebauer, P.; Deml, M. *J. Chromatogr., A* **1981**, *217*, 209−224.
(32) Kaniansky, D.; Marak, J. *J. Chromatogr., A* **1990**, *498*, 191−204.
(33) Krivankova, L.; Gebauer, P.; Bocek, P. *J. Chromatogr., A* **1995**, *16*, 35−48.
(34) Rogacs, A.; Marshall, L. A.; Santiago, J. G. *J. Chromatogr., A* **2014**, *1335*, 105−120.
(35) Garcia-Schwarz, G.; Rogacs, A.; Bahga, S. S.; Santiago, J. G. *J. Vis. Exp.* **2012**, *61*, e3890.
(36) Soengas, M. S.; Gutiérrez, C.; Salas, M. *J. Mol. Biol.* **1995**, *253*, 517−529.
(37) Reinhoud, N. J.; Tjaden, U. R.; van der Greef, J. *J. Chromatogr., A* **1993**, *641*, 155−162.
(38) Tu, J.; Ge, Q.; Wang, S.; Wang, L.; Sun, B.; Yang, Q.; Bai, Y.; Lu, Z. *BMC Genomics* **2012**, *13*, 43.
(39) Wu, Q.; Wang, C.; Lu, Z.; Guo, L.; Ge, Q. *Clin. Chim. Acta* **2012**, *413*, 1058−1065.

DOI: 10.1021/ac504406s
Anal. Chem. 2015, 87, 1404−1410

SUPPORTING INFORMATION

Highly-Sensitive Amplification-Free Analysis of Multiple miRNAs by Capillary Electrophoresis

David W. Wegman, Farhad Ghasemi, Anna Khorshidi, Burton B. Yang, Stanley K. Liu, George M. Yousef, and Sergey N. Krylov

Table of Contents

Page number

1. SUPPORTING MATERIALS AND METHODS

Table S1. List of target miRNAs, their nucleotide sequences, sequences of corresponding DNA hybridization probes and their respective peptide drag tags.

Name of sequence	miRNA Nucleotide sequence	Hybridization probe sequence with modifications	Peptide drag tag sequence
mir-125b	5'-CCU GAG ACC CUA ACU UGU GA-3'	5'-ThiolC6S-S-TCA CAA GTT AGG GTC TCA GGG A-Alexa488-3'	none
mir-155	5'-UUA AUG CUA AUC GUG AUA GGG GU-3'	5'-ThiolC6S-S-ACC CCT ATC ACG ATT AGC ATT AA-Alexa488-3'	C-term-Gly-Ala-Gly-Thr-Gly-N term
mir-21	5'-UAG CUU AUC AGA CUG AUG UUG A-3'	5'-ThiolC6S-S-TCA ACA TCA GTC TGA TAA GCT A-Alexa488-3'	C-term-Gly-Ala-Gly-Thr-Gly-Gly-Ala-Gly-Thr-Gly-N term
mir-10b	5'-UAC CCU GUA GAA CCG AAU UUG UG-3'	5'-ThiolC6S-S CAC AAA TTC GGT TCT ACA GGG TA-Alexa488-3'	C-term-Gly-Ala-Gly-Thr-Gly-Gly-Ala-Gly-Thr-Gly-Gly-Ala-Gly-Thr-Gly-N term
mir-145	5'-GUC CAG UUU UCC CAG GAA UCC CU-3'	5'-Thiol C6S-S-AGG GAT TCC TGG GAA AAC TGG AC-Alexa488-3'	C-term-Gly-Ala-Gly-Thr-Gly-Gly-Ala-Gly-Thr-Gly-Gly-Ala-Gly-Thr-Gly-Gly-Ala-Gly-Thr-Gly-N term

2. SUPPORTING RESULTS

2.1. Tables of quantum yields and DQAMmiR-measured miRNA concentrations

Table S2. Quantum yields of the DNA probes for the respective miRNA. q_P is the quantum yield of SSB-bound probe and q_H is the quantum yield of the DNA probe-miRNA hybrid. These values were determined as explained in our previous work.[27]

DNA Probe Type	MiR145 DNA probe	MiR10b DNA probe	MiR21 DNA probe	MiR-155 DNA probe	MiR125b DNA probe
q_P	0.24 ± 0.04	0.23 ± 0.03	0.37 ± 0.06	0.27 ± 0.05	0.22 ± 0.02
q_H	0.61 ± 0.08	0.62 ± 0.06	0.69 ± 0.08	0.63 ± 0.07	0.58 ± 0.06

Table S3. After the conjugation of peptides to the miRNA-specific DNA probes (peptide lengths of 5, 10, 15, and 20 amino acids were conjugated to the DNA probes for miR155, miR21, miR10b, and miR145, respectively), the variation of fluorescence intensity was taken into account. The fluorescence intensity of all DNA probes was normalized by determining their quantum yields (q_D) with respect to an untagged DNA probe (the untagged probe for miR125b was used as a reference).

DNA Probe Type	MiR145-20aa DNA probe	MiR10b-15aa DNA probe	MiR21-10aa DNA probe	MiR155-5aa DNA probe	MiR125b DNA probe
q_D	0.38 ± 0.02	0.58 ± 0.04	0.46 ± 0.02	0.47 ± 0.02	1

Table S4. Quantum yields of DNA probes conjugated to peptides upon binding to SSB (q_P') and upon hybridization with miRNA (q_H'). They were obtained by multiplying q_P and q_H by q_D

DNA Probe Type	MiR145-20aa DNA probe	MiR10b-15aa DNA probe	MiR21-10aa DNA probe	MiR155-5aa DNA probe	MiR125b DNA probe
q_P'	0.09 ± 0.02	0.13 ± 0.02	0.17 ± 0.03	0.13 ± 0.02	0.22 ± 0.02
q_H'	0.23 ± 0.03	0.36 ± 0.04	0.32 ± 0.04	0.29 ± 0.04	0.58 ± 0.06

Table S5. DQAMmiR-determined concentrations of the five miRNA (mir125b, mir155, mir21, mir10b, mir145) relative to their actual concentration as determined by light absorbance at 260 nm.

Actual miRNA Concentration (pM)	DQAMmiR-Determined miRNA Concentration (pM)				
	mir125	mir155	mir21	mir10b	mir145
1	1.24 ± 0.20	-	-	-	-
10	12.6 ± 4.6	11.0 ± 2.9	15.8 ± 3.9	11.1 ± 2.2	11.7 ± 4.9
50	58.8 ± 6.3	45.3 ± 4.2	57.4 ± 6.6	47.0 ± 9.1	47.2 ± 10
100	117 ± 6.8	85.0 ± 6.1	132 ± 8.1	86.4 ± 9.1	104 ± 16
500	565 ± 20	534 ± 53	486 ± 52	514 ± 24	515 ± 80
1000	991 ± 48	868 ± 96	926 ± 375	857 ± 126	1004 ± 65

2.2 Experimental results for the optimization of ITP-DQAMmiR

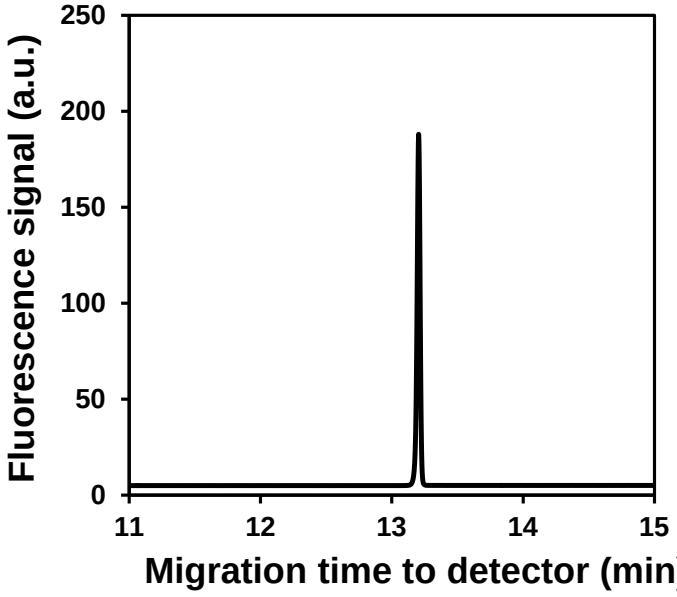

Figure S1. ITP concentration of all target analytes. A sample containing 1 nM mir125b, 155, 21, 10b and 145, 1 nM fluorescein and 10 nM of all 5 respective DNA-peptide probes was injected into a capillary. A voltage was applied and ITP was performed using using 50 mM Tris-Cl, pH 8.0 as LE and 20-10 mM Tris-HEPES, pH 8.3 as TE. All target analytes were concentrated into a narrow zone between the two buffers, as depicted by the sharp single peak.

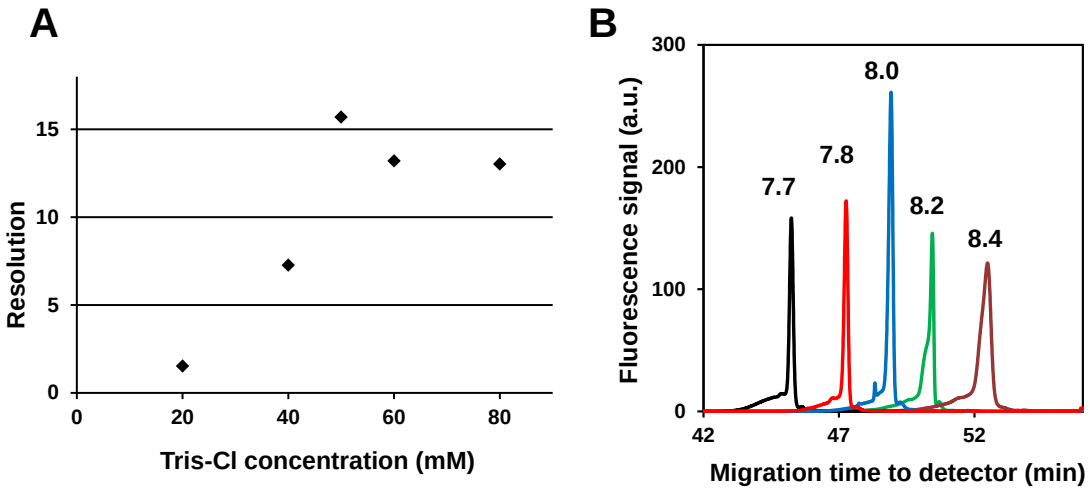

Figure S2. Optimization of LE concentration and pH. a) ITP-DQAMmiR was performed on a 1 nM 125 DNA, 1 nM fluorescein sample using an LE buffer with varying Tris-Cl concentration. Resolution between the fluorescein and DNA probe peak was measured. The greatest resolution occurred when using 50 mM Tris-Cl. b) ITP-DQAMmiR was performed on a 1 nM 125 DNA, 1 nM fluorescein sample using 50 mM Tris-Cl LE buffer with pH ranging from 7.7 – 8.4. The highest, sharpest peak (as well as greatest resolution, not shown) occurred with pH 8.0. It should be noted that TE was not optimized at this point, which explains the significant peak fronting.

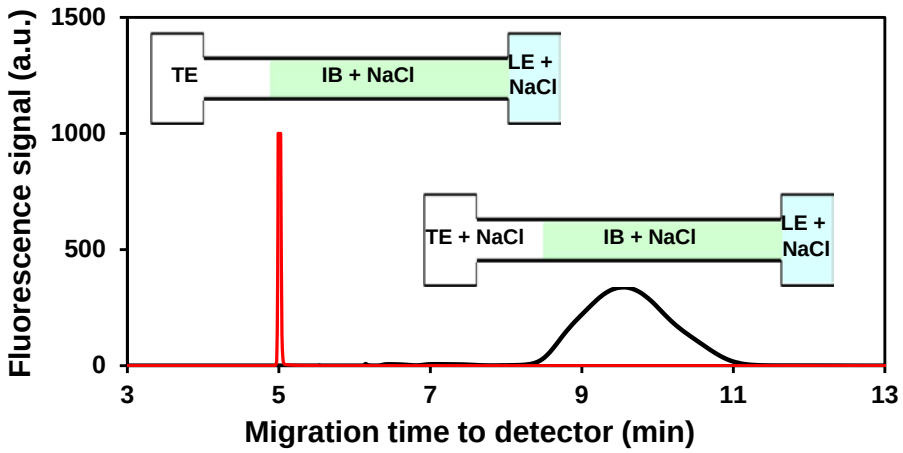

Figure S3. Inclusion of NaCl in LE and TE buffers. The 5 target miRNAs (mir125b, mir155, mir21, mir10b, mir155) and their respective DNA probes were hybridized in incubation buffer (IB) (20 mM Tris, 10 mM HEPES, 10 mM NaCl, pH 8.3). ITP runs were performed with 10 mM NaCl included in both LE and TE (black trace) or only LE (red trace). The presence of NaCl in both LE and TE (black trace) resulted in significant peak broadening. The presence of NaCl only in IB and LE resulted in a concentrated, narrow peak (red trace).

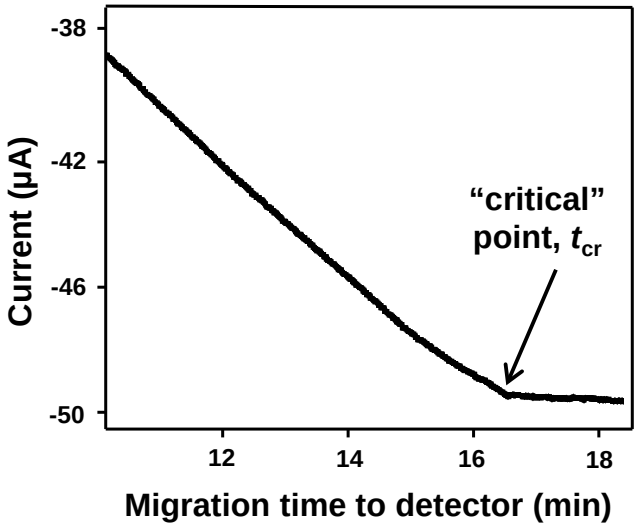

Figure S4. Determining the "critical" point, t_{cr}, of ITP-DQAMmiR. A current versus time plot is shown for a typical ITP-DQAMmiR run, focusing on the "critical" time-point. During ITP, the displacement of TE with LE is observed with a gradually increasing electrical current. ITP is run in the reverse direction, as such, the current is negative. The t_{cr}, is observed with an arrow, indicating the time where the slope abruptly changes from finite to zero.

Table S6. Reproducibility of critical ITP time point ($\boldsymbol{t_{cr}}$) over several days with different capillaries. ITP-DQAMmiR runs were performed using two different capillaries (#1 and #2) over several days. The time point at which the current *versus* time slope abruptly changes from finite to zero was recorded, and defined as the critical ITP time point ($\boldsymbol{t_{cr}}$).

Date of Experiment	**Capillary Used**	**"critical" ITP time-point, (t_{cr}) (min)**
Jan. 20, 2014	**#1**	**16.63**
Jan. 22, 2014	**#1**	**16.51**
Jan. 22, 2014	**#1**	**16.64**
Feb. 5, 2014	**#2**	**16.60**
Feb. 14, 2014	**#2**	**16.72**
Feb. 17, 2014	**#2**	**16.68**
	Mean ± Standard Deviation	**16.63 ± 0.07**

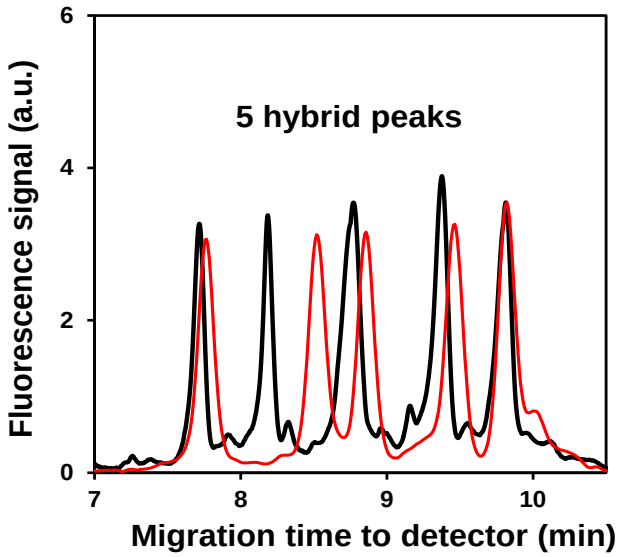

Figure S5. Separation of 5 hybrid peaks using ITP-DQAMmiR (red trace) and DQAMmiR (black trace). The 5 target miRNAs (mir125b, mir155, mir21, mir10b, mir155) were incubated with their respective DNA probes (containing 0, 5, 10, 15, and 20 amino acid drag tags respectively). Samples were injected into the capillary and were separated and detected using either ITP-DQAMmiR or DQAMmiR. ITP-DQAMmiR had a greater resolution between the 5 hybrid peaks than DQAMmiR. The ITP-DQAMmiR electropherogram was scaled-down and aligned to allow a qualitative comparison.

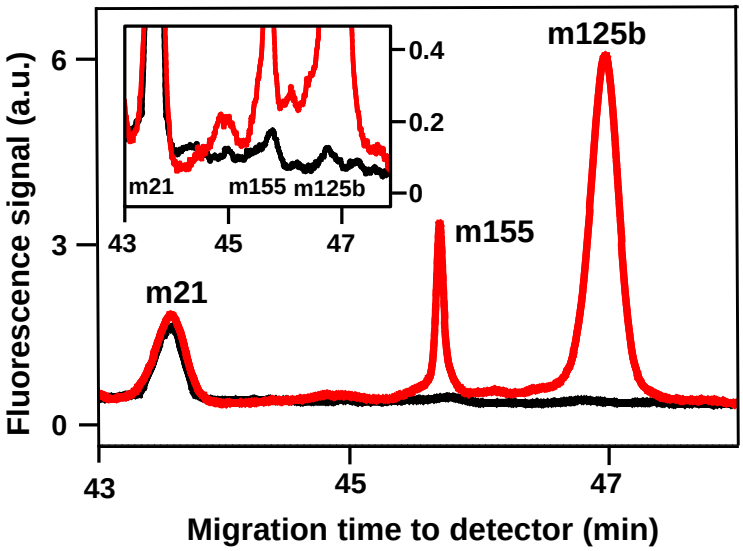

Figure S6. ITP-DQAMmIR analysis of multiple miRNAs spiked in to an RNA extraction sample. An MCF-7 RNA extract was incubated with 5 nM of the respective probes for miR125b, miR155, and miR21 with (red trace) or without (black trace) 300 pM of spiked-in mir12b5 and mir155. ITP-DQAMmiR was performed as previously explained. The detection of the spike-in miRNA peaks validates the detection of miRNA from the extract sample and allows us to conclude that the effects of the extract matrix on quantitation is negligible.

3. SUPPORTING MATHEMATICS (derivation of equation for the determination of concentrations of multiple miRNAs in DQAMmiR)

There was a misprint in the derivation of this equation with regards to the indices in our original work [27] which we correct here. The unknown concentration of the i-th miRNA, $[\text{miRNA}]_i$, can be expressed through the area of its respective hybrid peak ($A_{\text{H},i}$), using the unknown coefficient a and known quantum yield $q_{\text{H},i}$:

$$[\text{miRNA}]_i = a\left(A_{\text{H},i} / q_{\text{H},i}\right) \tag{S3-1}$$

The known concentration of the j-th probe, $[\text{P}]_{0,j}$ can be expressed through the areas of two peaks, the one of SSB-bound excess probe, $A_{\text{P},j}$, and the one of the miRNA-bound probe, $A_{\text{H},j}$, with the same coefficient a and known quantum yields $q_{\text{H},j}$ and $q_{\text{P},j}$:

$$[\text{P}]_{0,j} = aA_{\text{P},j} / q_{\text{P},j} + A_{\text{H},j} / q_{\text{H},j} \tag{S3-2}$$

Accordingly, the known total concentration of N DNA probes can be expressed using the following equation:

$$\sum_{j=1}^{N}[\text{P}]_{0,j} = a\left(\sum_{j=1}^{N} A_{\text{P},j} / q_{\text{P},j}\right) + a\left(\sum_{j=1}^{N} A_{\text{H},j} / q_{\text{H},j}\right) \tag{S3-3}$$

Since the peaks of the hybrids are resolved, their corresponding areas $A_{\text{H},j}$ can be experimentally determined; accordingly we treat them as known parameters. The peaks corresponding to the SSB-bound excess probes can, however, overlap. Therefore, we treat the areas corresponding to them, $A_{\text{P},j}$, as unknowns along with the coefficient a. While the individual $A_{\text{P},j}$ are unknown, their sum, A_{P}, can be experimentally measured and can thus be treated as a known parameter. To incorporate A_{P} in the equation, we need to isolate $A_{\text{P},j}$ from $q_{\text{P},j}$ by multiplying Equation S3-3 by $q_{\text{P},j}$:

$$\sum_{j=1}^{N} q_{\text{P},j}[\text{P}]_{0,j} = a\left(\sum_{j=1}^{N} A_{\text{P},j}\right) + a\left(\sum_{j=1}^{N}\left(q_{\text{P},j} / q_{\text{H},j}\right) A_{\text{H},j}\right) \tag{S3-4}$$

Equation S3-4 can be otherwise represented as:

$$\sum_{j=1}^{N} q_{\text{P},j}[\text{P}]_{0,j} = aA_{\text{P}} + a\left(\sum_{j=1}^{N}\left(q_{\text{P},j} / q_{\text{H},j}\right) A_{\text{H},j}\right) \tag{S3-5}$$

Now we can solve Equation S3-5 for a:

$$a = \frac{\sum_{j=1}^{N} q_{\mathrm{P},j}[\mathrm{P}]_{0,j}}{A_{\mathrm{P}} + \sum_{j=1}^{N}\left(q_{\mathrm{P},j} / q_{\mathrm{H},j}\right) A_{\mathrm{H},j}} \tag{S3-6}$$

By expressing a from Equation S3-1 and incorporating it into Equation S3-6 we get:

$$\frac{[\mathrm{miRNA}]_i q_{\mathrm{H},i}}{A_{\mathrm{H},i}} = \frac{\sum_{j=1}^{N} q_{\mathrm{P},j}[\mathrm{P}]_{0,j}}{A_{\mathrm{P}} + \sum_{j=1}^{N}\left(q_{\mathrm{P},j} / q_{\mathrm{H},j}\right) A_{\mathrm{H},j}} \tag{S3-7}$$

We can finally express the unknown concentration of the i-th miRNA in the following way:

$$[\mathrm{miRNA}]_i = \frac{A_{\mathrm{H},i}}{A_{\mathrm{P}} + \sum_{j=1}^{N}\left(q_{\mathrm{P},j} / q_{\mathrm{H},j}\right) A_{\mathrm{H},j}} \left(\sum_{j=1}^{N}\left(q_{\mathrm{P},j} / q_{\mathrm{H},i}\right)[\mathrm{P}]_{0,j} \right) \tag{S3-8}$$